



International Journal of Applied Sciences (IJAS)
Singaporean Journal of Scientific Research (SJSR)

Vol.7.No.1 2015 Pp.348-352

available at: www.iaaet.org/sjsr

Paper Received :25-12-2014

Paper Accepted:14-01-2015

Paper Reviewed by: 1Prof. L Selvakumar 2. Chai Cheng Yue

Editor : Dr. Chu Lio

TRAPPING FORCE NEAR A LASER-ILLUMINATED TAPERED GOLD TIP

M. Zohrabi, M. Kh. Salakhov, S. S. Kharintsev

Department of Optics and Nanophotonics, Institute of Physics, Kazan Federal University,
Kremlevskaya, 16, Kazan, 420008, Russia

Abstract

Optical near-fields are localized to the source region of optical radiation or to the surfaces of materials interacting with free radiation. Later work by Ashkin et al. led to the development of “optical tweezers”, devices which allow optical trapping and manipulating macroscopic particles and living cells with typical sizes in the range of 0.1 – 10 micrometers. Due to the high field gradients of evanescent waves, strong forces are predicted in optical near-fields. In this paper we used simulation FDTD method and compared the results of trapping force, both with tapered gold tip and without grating on a gold sphere with a 5 -nm diameter that to be put exactly under tip and see a 5- times increase in the optical forces exerted on particle in the new shape of gold tip.

Keywords: optical tweezers, Plasmon resonance, tapered gold tip.

1. Introduction

In many situations, optical near-fields are explored for their ability to localize optical energy to longitudinal scales smaller than the roughly diffraction limit of $\lambda/2$, where λ is the light wavelength. Discrete momentum transfer between photons (X-rays) and other particles (electrons) was shown experimentally by Compton in 1925 and the recoil momentum transferred from photons to atoms was

observed by Frisch in 1933 [1]. The mechanical force in laser trapping and cooling experiments can be understood on a semiclassical basis where the electromagnetic field is treated classically and the particle being trapped as a quantized two-level system [2]. However, the quantum theory of photons is used to interpret the results correctly [3]. Furthermore, according to the photon concept, there are quanta of energy and momentum transfer between the radiation field and the atom. The classical electrodynamics was used to derive the conservation law for linear momentum in an optical field. In the small object limit, a familiar expression was obtained for gradient and scattering forces. It is possible to derive the forces exerting on atoms and molecules in optical traps. This theory is applied to calculate the trapping forces near a laser illuminated metal tip. The net force exerted on an arbitrary object is determined by Maxwell’s stress tensor. [4] After an introduction to the theory of electromagnetic forces in section 2, a description of the Field-enhancement at a metal tip is given in section 3, where an interpretative value of electric field without grating and with tapered grating is explained. Then, the forces in optical near-fields and Optical tweezers are addressed in section 4. Finally, in section 5, discussion and conclusion is presented.

2. Theory of electromagnetic field forces

2-1. Maxwell’s stress tensor

The force \mathbf{F} on a charge q , moving with velocity \mathbf{v} in an external electromagnetic field in a medium that can be characterized by a permittivity ϵ and permeability μ , is given by $\mathbf{F} = q(\boldsymbol{\epsilon} + \mathbf{v}/c \times \mathbf{B})$, where \mathbf{E} and \mathbf{B} denote the electric field and the magnetic induction vectors, respectively. $\mathbf{B} = \mu\mathbf{H}$, where \mathbf{H} is the magnetic vector. In a system of charges the magnitude of total force equals the variation $d\mathbf{P}_{mec}/dt$ of the mechanical momentum of the system, assuming that [5, 6] we have the conservation law:

$$\frac{d\mathbf{P}_{mec}}{dt} + \frac{d\mathbf{P}_{field}}{dt} = \int_s \mathbf{T} \cdot \mathbf{n} ds \quad (1)$$

In (1) S is any arbitrary closed surface that includes a volume V which contains the system of charges; \mathbf{P}_{field} is the total electromagnetic momentum given $\mathbf{P}_{field} = \int_v \mathbf{S} dv/c^2$ [7], where c denotes the speed of light and $\mathbf{S} = c/4\pi(\boldsymbol{\epsilon} \times \mathbf{H})$ as the Poynting vector. \mathbf{T} is Maxwell's stress tensor, the components of which are given by

$$T_{ij} = \frac{1}{4\pi} [\epsilon \epsilon_i \epsilon_j + \mu \mathcal{H}_i \mathcal{H}_j - \frac{1}{2} \delta_{ij} (\epsilon \epsilon^2 + \mu \mathcal{H}^2)], \quad i, j = 1, 2, 3 \quad (2)$$

Therefore, modeling electromagnetic forces involves knowledge of the total field. Several procedures have been used to evaluate these fields in different configurations. The multiple-multipole method has been employed to find the force exerted by a near-infrared illuminated metal tip on a nanometric particle suspended in a liquid [8]. The coupled-dipole method was used to calculate the force from an illuminated flat dielectric surface on one or more particles [9, 10]. The integral method has been used to derive the force near a corrugated surface [11, 12].

2-2. The dipole approximation

Small particles with radius $a \ll \lambda$ respond to an external electromagnetic field with an induced dipole moment \mathbf{P} . Therefore, they experience the force [7]

$$\langle \mathbf{F} \rangle = \left\langle \frac{d\mathbf{P}_{mec}}{dt} \right\rangle = \int_s \langle \mathbf{T} \rangle \cdot \mathbf{n} ds \quad (3)$$

Let the external field be time-harmonic. By using the equations $\mathbf{P} = \text{Re}[\mathbf{p}(r)e^{-i\omega t}]$, $\mathbf{B} = \left(\frac{c}{i\omega}\right) \nabla \times \mathbf{E}$ and $\mathbf{p} = \alpha\mathbf{E}$, where α is the particle polarization, one can write the time-averaged force on the particle as [13]

$$\langle \mathbf{F}_j(r) \rangle = \frac{1}{2} \text{Re} \left[\alpha \mathbf{E}_k \frac{\partial \mathbf{E}_k^*(r)}{\partial x_j} \right], \quad j, k = 1, 2, 3 \quad (4)$$

The polarization of the small particle, including the radiation-reaction term is, $\alpha = \frac{\alpha_0}{1 - \frac{2}{3}ik^3\alpha_0}$

Where α_0 is the static polarization given by the Clausius-Mossotti equation, $\alpha_0 = \alpha^3(\epsilon - 1)/(\epsilon + 1)$ and $\epsilon = \epsilon_2/\epsilon_0$ is the ratio of the particle permittivity ϵ_2 to the surrounding medium ϵ_0 [14]. The wavenumber is $k = \sqrt{\epsilon_0}k_0$, where $k_0 = \omega/c$. For a

wave propagating along k , the electric-field vector can be written as

$$\mathbf{E}(r) = E_0(r)e^{ik \cdot r} \quad (5)$$

Substituting (5) into (3), one obtains the force experienced by a dipolar particle

$$\langle \mathbf{F} \rangle = \frac{1}{4} \text{Re}[\alpha] \nabla |E_0|^2 + \frac{1}{2} k \text{Im}[\alpha] |E_0|^2 - \frac{1}{2} \text{Im}[\alpha] \text{Im}[E_0 \cdot \nabla E_0] \quad (6)$$

where Im denotes the imaginary part. The first term is the gradient component of the force, whereas the second term shows the radiation-pressure contribution to the scattering force. In the case of a Rayleigh particle ($ka \ll 1$), by substituting the above approximation for α : $\alpha = \alpha_0 + \frac{2}{3} ik^3 |\alpha_0|^2$, the second contribution can also be expressed as [15]

$$\left(\frac{|E|^2}{8\pi}\right) C \frac{k}{k} \quad (7)$$

Where C is the particle scattering cross-section: $C = \frac{8}{3} \pi k^4 |\alpha_0|^2$. The last term in (2.8) is zero when the field has a single plane-wave component, as in the next case.

2-3. The force from an evanescent wave on a dipolar particle

Let the small particle be immersed in the electromagnetic field of an evanescent wave, electric vector of which is $E = Ae^{-qz}e^{iK \cdot R}$, where $r = (R, z)$ and $k = (K, k_z)$; K and k_z satisfy

$$K^2 + k_z^2 = K^2, \quad K^2 = \omega^2 - \epsilon_0/c^2, \quad \text{with } k_z = iq = I\sqrt{K^2 - k^2}.$$

We assume that this field is generated by total internal reflection (TIR) at a flat interface between two media of dielectric permittivity ratio $1/\epsilon$. The incident wave, s or p polarized (i.e. with the electric vector either perpendicular or in the plane of incidence), is influenced by the denser medium. Without any loss of generalizing, we can choose Oxz as the incidence plane, so that $K = (K, 0)$. Let t_\perp and t_\parallel be the transmission coefficients for s and p polarizations, respectively. The electric vector is

$$\mathbf{E} = (0, 1, 0)t_\perp e^{iKx}e^{-qz} \quad (8)$$

for s polarization, and

$$\mathbf{E} = (-iq, 0, K)\frac{t_\parallel}{k} e^{iKx}e^{-qz} \quad (9)$$

for p polarization.

By substituting the above expressions for the electric vector \mathbf{E} into (6), we readily obtain the total average force components. The scattering force is placed in the (x, y) -plane (that is, the plane contains the propagating wave vector of the evanescent wave), namely:

$$\langle \mathbf{F}_x \rangle = \frac{1}{2} |t|^2 k \text{Im}[\alpha] e^{-2qz} \quad (10)$$

While the gradient-force component, which is directed along Oz , is read as

$$\langle \mathbf{F}_z \rangle = -\frac{1}{2} |t|^2 q \text{Re}[\alpha] e^{-2qz} \quad (11)$$

In (10) and (11) t stands for either t_{\perp} or t_{\parallel} depending on whether the polarization is s or p, respectively. For an absorbent particle, by using (4) for α in (10) and (11), the scattering and absorption force is obtained

$$\langle F_x \rangle = \frac{1}{2} |t|^2 K e^{-2qz} \frac{\text{Im}[\alpha_0] + \frac{2}{3} k^3 |\alpha_0|^2}{1 + \frac{4}{9} k^6 |\alpha_0|^2} \quad (12)$$

and for the gradient force

$$\langle F_z \rangle = -\frac{1}{2} |t|^2 q \frac{\text{Re}[\alpha_0]}{1 + \frac{4}{9} k^6 |\alpha_0|^2} e^{-2qz} \quad (13)$$

It should be noted that, except for $\text{Re}[\epsilon]$ between -2 and 1 , $\text{Re}[\alpha_0]$ is positive, thus the gradient force is directed toward the interface. On the other hand, since $\text{Im}[\alpha_0]$ and $|\alpha_0|^2$ are always positive, the scattering force (12) pushes the particle in the direction of propagating K of the evanescent wave. Of course, these forces increase with a decrease in the distance from the interface, and are larger for p polarization due to the orientation of the induced polarization in the particle. [16] In particular, if $ka \ll 1$, (12) becomes

$$\langle F_x \rangle = \frac{1}{2} |t|^2 K e^{-2qz} \left[a^3 \text{Im} \left(\frac{\epsilon-1}{\epsilon+2} \right) \frac{2}{3} k^3 a^6 \left| \frac{\epsilon-1}{\epsilon+2} \right|^2 \right] \quad (14)$$

The first term of (14) is the radiation pressure of the evanescent wave on the particle due to its absorption, whereas the second term corresponds to scattering. This expression can be further compressed as

$$\langle F_x \rangle = \frac{|t|^2 K}{8\pi k} e^{-2qz} C_{\text{ext}} \quad (15)$$

where the particle extinction cross-section C_{ext} has been introduced as

$$C_{\text{ext}} = 4\pi K a^3 \text{Im} \left(\frac{\epsilon-1}{\epsilon+2} \right) + \frac{8}{3} \pi k^4 a^6 \left| \frac{\epsilon-1}{\epsilon+2} \right|^2$$

3. Field-enhancement at a metal tip

Field enhancement near Nanoscale metal structures plays a central (major) role in optical phenomena such as surface-enhanced Raman scattering (SERS), second-harmonic (SH) generation and near-field microscopy. The enhancement originates from the combination (integration) of the electrostatic lightning-rod effect, due to the geometric singularity of sharply pointed structures, and localized surface Plasmon resonances which depend sensitively on the excitation wavelength. The incident light drives the free electrons in the metal along the direction of polarization. While the charge density is zero inside the metal at any moment, charges accumulate on the surface of the metal. When the incidence polarization is perpendicular to the tip axis, diametrically opposed points on the tip surface have opposite charges. As a consequence, the foremost end of the tip remains uncharged and no field enhancement is achieved. On the other hand, when the incidence polarizations parallel to the tip axis, the induced surface charge density is almost rotationally symmetric and has a highest amplitude at the end of the tip [17, 18, 19]. Enhanced field is confined (restricted) to the tip apex in all

three dimensions. Thus the illuminated tip represents a nanoscale light source. The maximum enhancement of the electric field intensity $M = |E_{\text{local}}(r, \omega)|^2 / |E_{\text{in}}(r, \omega)|^2$ calculated for a solid gold tip with a diameter of 10 nm at an excitation wavelength of 830 nm is around (about) 250. To establish (generate) a strong field enhancement at the tip, the electric field of the exciting laser beam needs to be polarized along the tip axis. The influence of tip shape and material on the field enhancement has been discussed in a series of publications with the aim to find the optimum tip [20, 21]. In this work, we investigated the influence of tip shape on the field enhancement. We assumed a golden tip, a 10 - nm radius of apex and a 30° cone angle and a 200 - nm period of grating. Also we used continuous laser with a wavelength in the range 400 nm to 700 nm. We simulated in two different conditions. We considered direct illumination apex tip without grating and direct illumination of grating. Spherical gold particle was put under apex tip in a distance of 3 nm. The figures 1 and 2 show electric field around of apex tip without grating and with tapered grating, respectively.

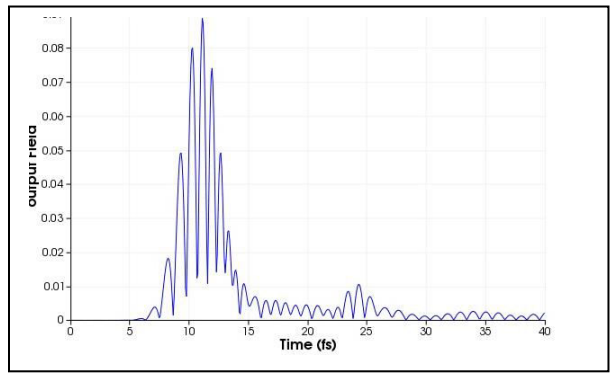
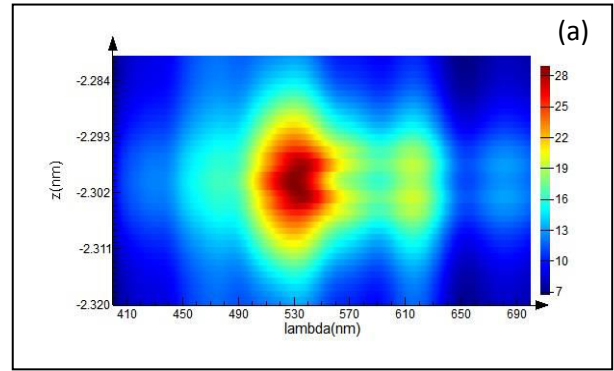


Fig.1, Enhancement electric field without grating in the around of apex tip, (a) in direction axes z for different wavelength and (b) in terms of time.

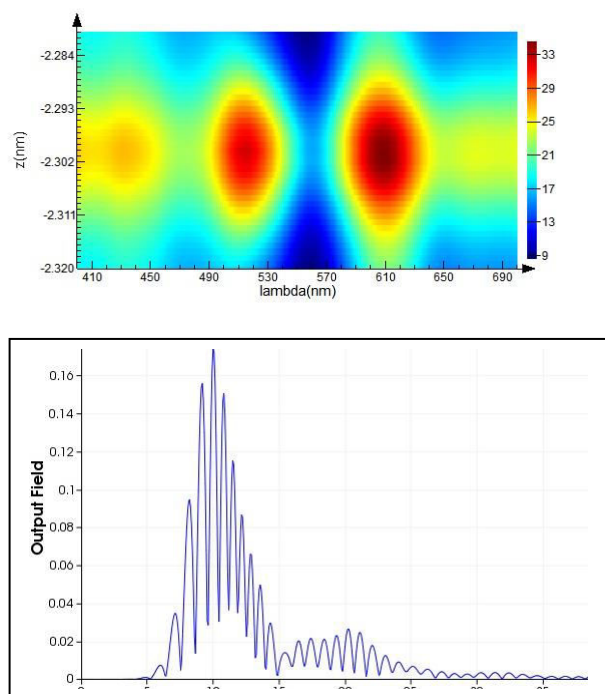


Fig. 2, enhancement electric field with tapered grating in the tip apex, (a) in direction axes z for different wavelength and (b) in terms of time.

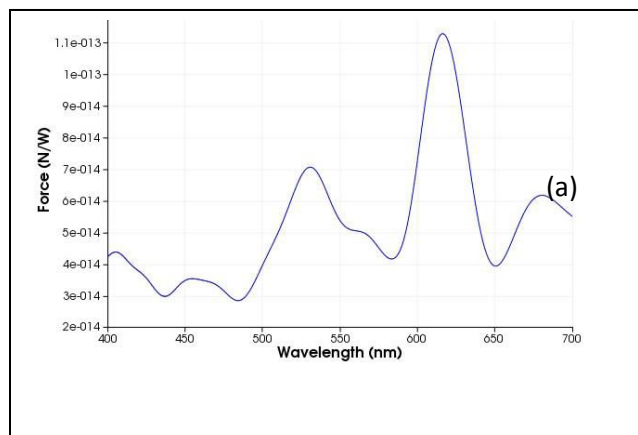
As illustrated in Fig. 2, intensity of electric field is increased with grating in the tip apex. Also we see that without grating tip, maximum electric field is generated at around 530 nm but with grating tip, it is generated at around 610 nm. The reason for wavelength change is excitation Surface Plasmon.

4. Forces in optical near-fields and Optical tweezers

In principle, optical tweezers rely upon an extremely high gradient in the electric field produced near the beam waist of a tightly focused laser beam, which generates a force sufficient to trap micron-sized dielectric particles in three dimensions. In 1986 Ashkin, et. al. showed that a single tightly focused laser beam could be used to hold, in three dimensions, a microscopic particle near the beam focus. This has now become established as a powerful noninvasive technique and is known as optical tweezers [22]. Optical tweezers have found widespread application especially in biology and have been used to manipulate dielectric spheres, and metallic particles. Optical tweezers are routinely applied to measure elasticity, force, torsion and position of a trapped object. Forces measured with optical tweezers are typically in the 1 – 10pN range. A simple ray optical analysis can be applied to describe trapping of particles larger than the wavelength. In this model, every refraction of alight ray at the particle surface

transfers (moves)with momentum from the trapping laser to the particle. The time rate of change of the momentum is the trapping force. The total force can be calculated by representing the light beam as a collection of rays, and summing the forces from each of the rays up. Stable trapping requires that there exist a position for which the net force on the particle is zero and any displacement results in a restoring force towards the ‘zero-force’ position [23].The enhanced field at the tip results from an increase in the surface charge density. The incident light drives the free electrons in the metal along the direction of polarization. While the charge density is zero inside the metal at any instant of time ($\nabla \cdot E = 0$), charges accumulate on the surface of the metal. When the incidence polarization is perpendicular to the tip axis, diametrically opposed points on the tip surface have opposite charges. As a consequence, the foremost end of the tip remains uncharged. On the other hand, when the incidence polarization is parallel to the tip axis the induced surface charge density is rotationally symmetric and has the highest amplitude at the end of the tip. In both cases the surface charges form a standing wave oscillating with the frequency of the excitation light but with wavelengths shorter than the wavelength of the exciting light (Surface Plasmon) [4].

In our simulation, optical forces by tapered gold tip exerted on one spherical gold particle with a 5 -nm diameter in terms of wavelength are increased approximately 5 times. As shown in Fig. 4, optical force in wavelength is increased around 620 nm.



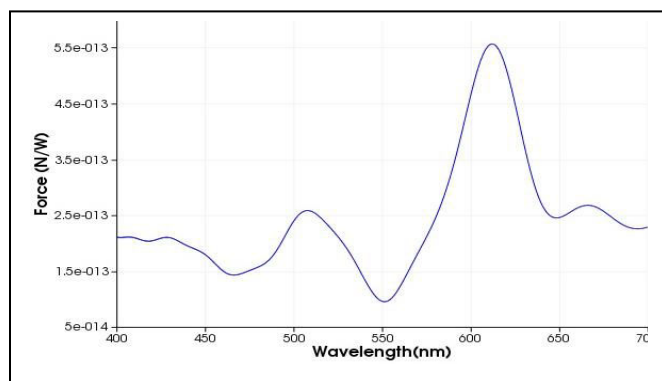


Fig. 4, Optical forces by tip, (a) without and (b) with grating exerted on one metal spherical with 5 nm diameters in terms of wavelength, respectively. We see a 5- times increase in the force of wavelength around 620 nm.

5. Conclusion

Since the first realization that radiation pressure could be used to manipulate matter (the materials), the applications of photonic forces have ranged from laser cooling and trapping of atoms and molecules to manipulation and assembling of small particles and biological systems. With the advent of near-field optics and nanophotonics, the possibility of shaping optical fields on the sub-wavelength scale has opened a new realm of applications for photonic forces: a domain where evanescent modes of the electromagnetic fields prevail and where light can be confined to nanometric regions. We propose in this paper a new shape for tip. Our concept is demonstrated with the 3D trapping of a piece of 10- nm spherical gold. Comparative numerical analysis of the optical forces induced by the laser on gold tip with and without grating enhances 5 times trapping force around tapered tip.

Acknowledgment

The authors wish to thank prof .R. H. Gajnutdinov, for help full discussions. We are also grateful Department of Optics and Nanophotonics, Kazan Federal University to for giving us access to their equipment.

References

[1] R. Frisch, "Experimenteller Nachweis des Einsteinischen Strahlungsdruckstosses," *Z.Phys.* **86**, 42–45 (1933).
 [2] Y. Shimizu and H. Sasada, "Mechanical force in laser cooling and trapping," *Am. J.Phys.* **66**, 960–967 (1998).
 [3] S. Stenholm, "The semiclassical theory of laser cooling," *Rev. Mod. Phys.* **58**, 699–739 (1986).
 [4] L. Novotny and B.Hecht 2006 "Principles of Nano-Optics" Cambridge
 [5] Jackson, J. D. 1975 Classical electrodynamics. Wiley.
 [6] Stratton, J. A. 1941 Electromagnetic theory. New York: McGraw-Hill.

[7] Gordon, J. P. 1973 Radiation forces and momenta in dielectric media. *Phys. Rev.* **A8**, 14–21.
 [8] Novotny, L., Bian, R. X. & Xie, X. S. 1997 Theory of nanometric optical tweezers. *Phys. Rev. Lett.* **79**, 645–648.
 [9] Chaumet, P. C. & Nieto-Vesperinas, M. 2000a Coupled dipole method determination of the electromagnetic force on a particle over a flat dielectric substrate. *Phys. Rev.* **B61**, 14 119– 14 127.
 [10] Chaumet, P. C. & Nieto-Vesperinas, M. 2000b Electromagnetic force on a metallic particle in the presence of a dielectric surface. *Phys. Rev.* **B62**, 11 185–11 191.
 [11] Lester, M., Arias-Gonzalez, J. R. & Nieto-Vesperinas, M. 2001 Fundamentals and model of photonic-force microscopy. *Opt. Lett.* **26**, 707–709.
 [12] Arias-Gonzalez, J. R., Nieto-Vesperinas, M. & Lester, M. 2002 Modeling photonic force microscopy with metallic particles under plasmon excitation. *Phys. Rev.* **B65**, 115 402.
 [13] Chaumet, P. C. & Nieto-Vesperinas, M. 2000c Time-averaged total force on a dipolar sphere in an electromagnetic field. *Opt. Lett.* **25**, 1065–1067.
 [14] Draine, B. T. 1988 The discrete dipole approximation and its application to interstellar graphite grains. *Astrophys. J.* **333**, 848–872.
 [15] Van de Hulst, H. C. 1981 Light scattering by small particles. New York: Dover.
 [16] M. Nieto-Vesperinas, P. C. Chaumet, A. Rahmani. 2004 Near-field photonic forces. *Phil. Trans. R. Soc. Lond.A* **362**, 719–737.
 [17] Larsen, R. E. & Metiu, H. 2001 Resolution and polarization in apertureless near-field microscopy. *J. Chem. Phys.* **114**, 6851–6860.
 [18] Martin, Y. C., Hamann, H. F. & Wickramasinghe, H. K. 2001 Strength of the electric field in apertureless near-field optical microscopy. *J. Appl. Phys.* **89**, 5774–5778.
 [19] Novotny, L., Sánchez, E. J. & Xie, X. S. 1998 Near-field optical imaging using metal tips illuminated by higher-order Hermite–Gaussian beams. *Ultramicroscopy* **71**, 21–29.
 [20] Krug, J. T. I., Sánchez, E. J. & Xie, X. S. 2002 Design of near-field probes with optimal field enhancement by finite difference time domain electromagnetic simulation. *J. Chem. Phys.* **116**, 10 895–10 901.
 [21] Martin, Y. C., Hamann, H. F. & Wickramasinghe, H. K. 2001 Strength of the electric field in apertureless near-field optical microscopy. *J. Appl. Phys.* **89**, 5774–5778.
 [22] A. Ashkin, "Optical trapping and manipulation of neutral particles using lasers," *Proc. Natl. Acad. Sci. USA* **94**, 4853–4860 (1987).
 [23] A. Ashkin, "Forces of a single-beam gradient laser trap on a dielectric sphere in the ray optics regime," *Biophys. J.* **61**, 569–582 (1992).